Molecular Beam Magnetic Resonance Spectra of $TlCl^{35}$ and $TlCl^{37}$ at Zero Field*

H. J. ZEIGER† AND D. I. BOLEF
Columbia University, New York, New York
(Received October 17, 1951)

The molecular beam magnetic resonance method has been used to investigate the spectra of $TlCl^{35}$ and $TlCl^{37}$ at zero field. A splitting of the quadrupole line for both isotopes is observed and is attributed to a cosine coupling of the form $c_a\mathbf{I}\cdot\mathbf{J}$, between the chlorine spin $\mathbf{I}_a$ and the rotational angular momentum of the molecule $\mathbf{J}$.

It is assumed that the gradient of the electric field at the position of the chlorine nucleus q is a function of the internuclear distance R of the form

$$q(R)=q^{(0)}+q^{(1)}[(R-R_e)/R_e]+q^{(2)}[(R-R_e)/R_e]^2+\cdots$$

where R_e is the equilibrium value of R in the zeroth vibrational and rotational state ($v=0$, $J=0$). The average of $q(R)$ over the vibration and rotation of the molecule is shown to lead to a v and J dependence of the quadrupole coupling eqQ of the form

$$eqQ=e\bar{q}Q+eq^{(J)}QJ(J+1)+eq^{(v)}Qv.$$

The variation of eqQ with v and J explains the asymmetry observed in the TlCl line shapes.

The energy levels and transition frequencies are calculated for TlCl, a heteronuclear diatomic molecule with one nucleus having a quadrupole coupling with v and J dependence, and a cosine coupling with $\mathbf{J}$; and the second nucleus having a cosine coupling with $\mathbf{J}$. A detailed analysis of the line shape is presented.

The results for Cl^{35} in $TlCl^{35}$ are: $|e\bar{q}Q|/h=15.788\pm0.02$ Mc, $|eq^{(v)}Q|/h=96$ kc, $|eq^{(J)}Q|/h=18.4$ cps, $|c_a|/h=1.4\pm0.1$ kc. The results for Cl^{37} in $TlCl^{37}$ are: $|e\bar{q}Q|/h=12.425\pm0.02$ Mc, $|eq^{(v)}Q|/h=76$ kc, $|eq^{(J)}Q|/h=16.4$ cps, $|c_a|/h=1.1\pm0.1$ kc. $eq^{(v)}Q$ and $eq^{(J)}Q$ are shown to have the same sign as $e\bar{q}Q$ for both $TlCl^{35}$ and $TlCl^{37}$.

The zero field lines for Na^{23} in $Na^{23}F$ and $Na^{23}Cl$ are also discussed and are analyzed using the same theory. The results for Na^{23} in $Na^{23}Cl$ are: $|e\bar{q}Q|/h=5.608\pm0.02$ Mc, $|eq^{(v)}Q|/h\sim88$ kc, $|eq^{(J)}Q|/h\sim24$ cps, $|c_a|/h\sim1$ kc. The results for Na^{23} in $Na^{23}F$ are: $|e\bar{q}Q|/h=8.40\pm0.02$ Mc, $|eq^{(v)}Q|/h\sim80$ kc, $|eq^{(J)}Q|/h\sim32$ cps, $|c_a|/h\sim1$ kc. The signs of $eq^{(v)}Q$ and $eq^{(J)}Q$ are shown to be opposite to the sign of $e\bar{q}Q$ for both $Na^{23}Cl$ and $Na^{23}F$.

I. INTRODUCTION

THE molecular beam magnetic resonance method[1–3] has been used extensively in the investigation of nuclear and molecular properties of diatomic molecules. In determining the quadrupole interaction constants of diatomic molecules, the method of "zero field" has been found of particular value. In this method, the homogeneous magnetic field in which transitions occur is reduced to zero. The zero field technique has been applied successfully by Nierenberg and Ramsey[4] in the determination of the quadrupole interaction constants of NaBr, NaCl, and NaI. The positions of the lines at zero field agreed with those predicted from the high field spectrum, in agreement with the theory of Feld and Lamb.[5] However, the lines were unexpectedly broad (150–200 kc half-width), and showed a marked asymmetry in shape.

Nierenberg and Ramsey attributed the line broadening to a cosine coupling, $c\mathbf{I}\cdot\mathbf{J}$, between the nuclear spin of sodium $\mathbf{I}$ and the rotational angular momentum of the molecule $\mathbf{J}$. It will be shown in the discussion to follow that the addition of this term to the Hamiltonian should cause a splitting of the zero field quadrupole line. That the splitting was not observed in the case of the sodium halides, Nierenberg and Ramsey attributed to a dependence of the quadrupole coupling eqQ on the vibrational quantum number v and rotational quantum number, J. As shown in Appendix III, this dependence is expected to be of the form $eqQ=e\bar{q}Q+eq^{(J)}QJ(J+1)+eq^{(v)}Qv$, where $q^{(J)}$ and $q^{(v)}$ are very much smaller than $\bar{q}$, and all three are independent of $\mathbf{J}$ and v. The spectrum observed is due to transitions between the quadrupole hyperfine structure components within a given state characterized by v and J. The transition frequencies then have a slight v and J dependence which, in the case of the sodium halides, masks the $\mathbf{I}\cdot\mathbf{J}$ splitting and causes a line asymmetry. In the case of TlCl, the v and J dependence leads to an asymmetry in the shape of the line which has been split by the $\mathbf{I}\cdot\mathbf{J}$ interaction.

In this investigation, the method of zero field has been applied not only to the determination of the quadrupole interaction constant, but also to the determination of the constants c, $eq^{(J)}Q$, and $eq^{(v)}Q$ for Cl in the molecules $TlCl^{35}$, $TlCl^{37}$; and for Na^{23} in the molecules $Na^{23}F$ and $Na^{23}Cl$. The signs of $eq^{(J)}Q$ and $eq^{(v)}Q$ are determined relative to the sign of $e\bar{q}Q$. Because the transition frequencies have only a slight v and J dependence through $eq^{(J)}QJ(J+1)$ and $eq^{(v)}Qv$, it is necessary to analyze statistically the envelope of a large number of unresolved lines in order to obtain the desired values of these nuclear and molecular constants.

These finer molecular effects on the quadrupole hyperfine structure are of interest for their contribution to the understanding of the internal interactions in a diatomic molecule. They are also of value in increasing the precision with which the quadrupole interaction constant can be measured.

* This research has been supported in part by the ONR.
† Submitted by H. J. Zeiger in partial fulfillment of the requirements for the degree of Doctor of Philosophy in Physics at Columbia University.
[1] Rabi, Millman, Kusch, and Zacharias, Phys. Rev. **55**, 526 (1939).
[2] Kellogg, Rabi, Ramsey, and Zacharias, Phys. Rev. **56**, 728 (1939).
[3] J. M. B. Kellogg and S. Millman, Revs. Modern Phys. **57**, 677 (1940).
[4] W. A. Nierenberg and N. Ramsey, Jr., Phys. Rev. **72**, 1075 (1947).
[5] B. T. Feld and W. E. Lamb, Jr., Phys. Rev. **67**, 15 (1945).

II. APPARATUS AND METHOD

The apparatus is essentially one built by Kusch and Millman[1] and used later by Nierenberg and Ramsey in their experiments on the sodium halides. Data on construction, strength of deflecting fields, and other details may be found in references 1 and 4. For the substances used in this experiment, a beam of molecules is obtained at an elevated temperature (~1000°K) in the hot oven source. At this temperature, a large number of rotational states are excited. For example, the most probable value of J for TlCl is 55.

To generate the large radiofrequency currents needed for the oscillating field, a modified form of the Hartley oscillator was used. By the use of interchangeable tank components, it was found possible to maintain oscillations with rf output currents up to 20 amperes in the frequency range from 5 to 3000 kc. Above 3000 kc, another similar oscillator designed for higher frequencies was used.

The rf current from the generator passed through the homogeneous C-field region in water-cooled twin copper sheets 1.9 cm wide, 7 cm long, and $\frac{1}{16}$ in. thick, separated by Lavite spacers so as to leave a gap $\frac{1}{16}$ in. wide down the center of the C-field. Lavite spacers were also used to prevent the hairpin (as the rf magnetic field assembly is often called) from shorting to the pole faces of the C-field. A current of 1 ampere through the hairpin gave rise to a field of 1.7 gauss in a direction perpendicular to the C-field and to the direction of the beam.

Frequency measurements at low frequency were made on a General Radio precision wavemeter, type 724B. Intermediate and high frequency measurements were made on a General Radio heterodyne meter, type 620A, with which frequency can be measured to better than 0.005 percent. Both instruments, within the range in which they were used, provide a degree of precision higher than the limits imposed by other factors which determine line positions.

Since all the data were taken at zero field, it was not necessary to measure the value of the magnetic C-field. It was, however, necessary to develop a procedure for obtaining zero field. The demagnetization procedure adopted was applied before an experimental run was made, and the fact that the results of several runs on the same resonance minima agreed so closely was taken to be adequate proof of the consistency of the demagnetization procedure. The value of the field after demagnetization was estimated as less than 4 gauss. The application of a very small dc field, less than 10 gauss, was found, as is to be expected from the Feld-Lamb theory, to have negligible effect on both the position and intensity of the resonance lines. The broadening of the zero field line by a small dc field is also predicted by the theory, but the broadening in this experiment is less than that due to the oscillating field.

By line intensity we mean the change in total beam produced by the application of the oscillating field.

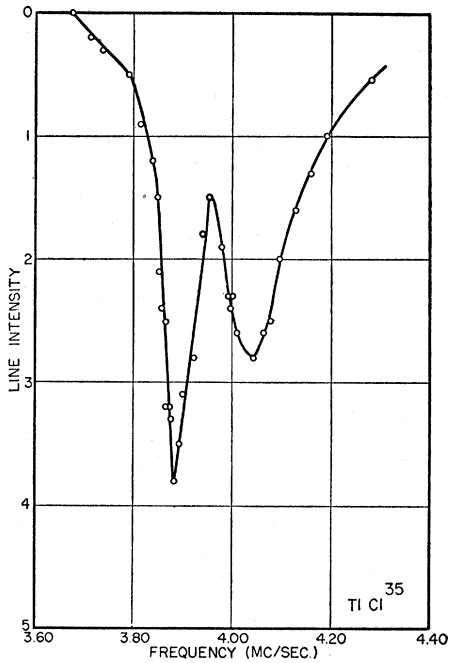

FIG. 1. Zero field spectrum of Cl^{35} in $TlCl^{35}$. Line intensity (decrease of beam at the detector) is expressed in cm deflection on a galvanometer scale. Peak intensity corresponds to a 0.5 percent decrease in total beam. Radiofrequency current was 12 amperes. The width of the line at half-intensity of each component is ~100 kc, considerably greater than the 3 kc resolution half-width of the apparatus for this molecule.

Because of the v and J dependence of the transition frequency, only a small number of states take part in the transition at a particular frequency. For this reason, the line intensity observed was small (about 1 percent of the total beam). In practice, values of the rf current were used which gave maximum line intensity without obscuring the details of the spectrum. Lowering the rf in most cases resulted in a decrease in line intensity without any observable decrease of line half-width or increase of resolution of two neighboring lines.

Due to sharply varying magnetic fields in the C-field region, nonadiabatic transitions[6] may occur between the A and B fields when the C-field is zero. Under these circumstances, the line intensity decreases because of a decrease in the number of space quantized molecules available for transition. To test whether the apparatus used in these experiments was free of such difficulties, the refocused beam intensity under normal high field conditions was compared with the beam intensity when the C-field was reversed with respect to the A and B fields. The loss in beam intensity was only a few percent, indicating a negligible loss in beam due to nonadiabatic transitions.

III. EXPERIMENTAL DATA

Neglecting all internal magnetic interactions and the variation of eqQ with v and J, one expects to see, for

[6] E. Majorana, Nuovo cimento 9 (1932).

the zero field spectrum of a heteronuclear molecule, a single resonance line whose width is given by rf broadening alone. The frequency at which this line appears would correspond to the quadrupole transition energy, which, in the case of spin $\frac{3}{2}$, is given by $\Delta W = eqQ/4$, where eqQ is the usual quadrupole coupling.[7]

It is evident from Figs. 1–4, showing the zero field spectra of Cl^{35} in $TlCl^{35}$, Cl^{37} in $TlCl^{37}$, Na^{23} in $Na^{23}F$, and Na^{23} in $Na^{23}Cl$, that other effects enter to change the shape of the curves. These effects have already been mentioned briefly and will be discussed more fully in the next section.

Since thallium has a spin of $\frac{1}{2}$, and hence no quadrupole moment, one expects to see, at zero field, quadrupole resonance lines corresponding only to the quadrupole interaction of Cl^{35} and Cl^{37} in TlCl. From Figs. 1 and 2, it can be seen that both lines are split into two components of marked asymmetry, the high frequency component being considerably broadened as compared with the low frequency component. The low frequency component is also seen to rise much more sharply than the high frequency component, the latter, indeed, tapering off very gradually to high frequencies. The width at half intensity of either component, of the order of 100 kc, is much greater than the resolution half-width of the apparatus, which is of the order of 3 kc for TlCl. Broadening due to the large rf currents, approximately 10 kc, is also too small to explain the large half-widths of the components. The ratio of the intensities of the Cl^{35} and Cl^{37} resonances is explained on the basis of relative abundance, and the difference in throwout power due to the difference in values of the nuclear g-factors. For both isotopes of chlorine, the ratio of the intensities of the split peaks is, on the average, equal to 1.7, while the ratio of the half-widths is 0.72. The splitting for the case of Cl^{35} is 156 kc; for Cl^{37}, 105 kc.

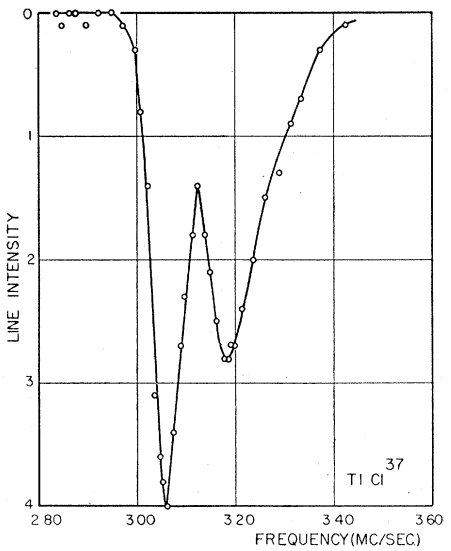

FIG. 2. Zero field spectrum of Cl^{37} in $TlCl^{37}$. Peak intensity corresponds to a 0.3 percent decrease in the total beam. The ratio of the half-widths of the split lines and the ratio of the intensities of the two wings are approximately the same as those of Fig. 1. Radiofrequency current was 15 amperes.

[7] J. Bardeen and C. H. Townes, Phys. Rev. **73**, 97 (1948).

The values of these constants for both Cl isotopes in TlCl are obtained from a weighted average of data from a number of curves taken under varying experimental conditions. It was found necessary to take a large volume of data primarily because the line intensity never exceed a value of 0.5 percent of the total beam.

The general features exhibited by the resonance curves in Figs. 3 and 4 (Na^{23} in $Na^{23}F$ and $Na^{23}Cl$, respectively) are the same as those of the resonance curves in Figs. 1 and 2, although in the case of Na the splitting is not as prominent, the components being barely resolved in the case of NaCl. For the Na resonances, the high frequency approach to the resonance minimum is sharp, while the low frequency end trails off very gradually, which is opposite to the case of TlCl. In the case of NaF, the ratio of the peak intensities is 1.2; in the case of NaCl it is 1.4. The separation between peaks for NaF is 60 kc; for NaCl it is 88 kc. The ratio of the half-width of the composite line to the splitting is 2.4 in the case of NaF; in the case of NaCl it is 2.0.

IV. THEORY

A. Hamiltonian and Transition Energies

The Hamiltonian operator which best explains the observed magnetic resonance spectra of $TlCl^{35}$ and $TlCl^{37}$ at zero field is:

$$\mathcal{H}=\frac{-eq(R)Q}{2I_a(2I_a-1)(2J+3)(2J-1)}\times\{3(\mathbf{I}_a\cdot\mathbf{J})^2+\tfrac{3}{2}(\mathbf{I}_a\cdot\mathbf{J})-I_a(I_a+1)J(J+1)\}+c_a(\mathbf{I}_a\cdot\mathbf{J})+c_b(\mathbf{I}_b\cdot\mathbf{J}). \quad (1)$$

The first term is the electric quadrupole interaction between the chlorine nucleus and the molecular charge external to the chlorine nucleus.[7,8] Q is the electric quadrupole moment of the chlorine nucleus, and $q(R)$ is the gradient, at the position of the chlorine nucleus, of the electric field along the internuclear axis, due to all the molecular charge external to the chlorine nucleus. $q(R)$ is assumed to be a function of internuclear distance R and will be discussed further under Sec. B and in Appendix III. The second term is a cosine coupling between the spin $\mathbf{I}_a$ of the chlorine nucleus and the rotational angular momentum of the molecule.[9] The third term is a cosine coupling between the spin $\mathbf{I}_b$ of the thallium nucleus and $\mathbf{J}$. This last term is necessary to explain the electric resonance spectra of $TlCl^{35}$ and

[8] H. B. G. Casimir, Teyler's Tweede Genootschap, 1936.

[9] H. M. Foley, Phys. Rev. **72**, 504 (1947); G. C. Wick, Phys. Rev. **73**, 51 (1948).

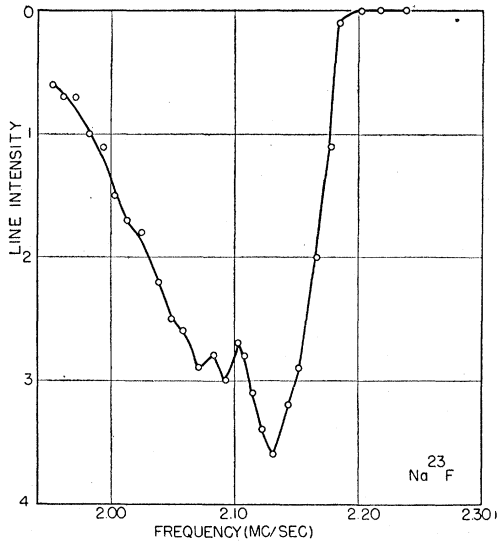

FIG. 3. Zero field spectrum of Na^{23} in $Na^{23}F$. Peak intensity corresponds to a 3-percent decrease in total beam. Radiofrequency current was 20 amperes.

$TlCl^{37}$, but will be shown in Appendix II to have a negligible effect on the spectra observed in this experiment. The effects of matrix elements of the quadrupole operator off-diagonal in J are also considered in Appendix II and are shown to be small.

Since the quadrupole coupling of $\mathbf{I}_a$ to $\mathbf{J}$ is much stronger than the cosine coupling of $\mathbf{I}_b$ to $\mathbf{J}$, the appropriate representation in which to discuss the energy levels due to (1) is the $(J, I_a, F_1, I_b, F, M_F)$ representation.[10] In this representation, $\mathbf{I}_a$ and $\mathbf{J}$ couple to give $\mathbf{F}_1$, and $\mathbf{F}_1$ couples with $\mathbf{I}_b$ to give $\mathbf{F}$. M_F is the component of $\mathbf{F}$ on the field direction.

The Hamiltonian can be written as the sum of a large part, $\mathcal{H}_0$, which is diagonal in this representation, and a small part, $\mathcal{H}_1$, which is not diagonal, as follows:

$$\mathcal{H}_0=\frac{-eq(R)Q}{2I_a(2I_a-1)(2J+3)(2J-1)}\times\{3(\mathbf{I}_a\cdot\mathbf{J})^2+\tfrac{3}{2}(\mathbf{I}_a\cdot\mathbf{J})-I_a(I_a+1)J(J+1)\}+c_a(\mathbf{I}_a\cdot\mathbf{J})+c_b(\mathbf{I}_b\cdot\mathbf{F}_1) \quad (2)$$

$$\mathcal{H}_1=-c_b(\mathbf{I}_b\cdot\mathbf{I}_a).$$

$\mathcal{H}_0$ gives energy levels nondegenerate in F_1 and F, but degenerate in M_F. However, because $(\mathbf{I}_b\cdot\mathbf{I}_a)$ does not connect states of different M_F, nondegenerate perturbation theory may be used to obtain the contribution of $\mathcal{H}_1$ to the energy levels.[11] The energy levels obtained when $I_a=\frac{3}{2}$, $I_b=\frac{1}{2}$ (the case for $TlCl^{35}$ and $TlCl^{37}$) are given in Appendix I.

Transitions are produced by an oscillating magnetic field at right angles to the direction of motion of the beam, as in the usual molecular beam magnetic resonance experiments.[1-3] The selection rules for the spectra observed in this experiment are: $\Delta F=+1$, $\Delta F_1=+1$, $\Delta M_F=\pm1$; or $\Delta F=-1$, $\Delta F_1=-1$, $\Delta M_F=\pm1$. These correspond to a reorientation of spin $\mathbf{I}_a$ with respect to $\mathbf{J}$, and no reorientation of spin $\mathbf{I}_b$; they are then essentially the same as the zero field selection rules $\Delta F=\pm1$, $\Delta M_F=\pm1$ for the case of a single nuclear spin $\mathbf{I}$ coupled to $\mathbf{J}$ to give the resultant $\mathbf{F}$.

Application of these selection rules leads to the transition energies for the case $I_a=\frac{3}{2}$, $I_b=\frac{1}{2}$,

$$W(F_1=J+\tfrac{3}{2}\leftrightarrow F_1=J+\tfrac{1}{2})=-\frac{eq(R)Q}{4}+c_a(J+\tfrac{3}{2})+\frac{3c_b}{4J}-\frac{3[1\mp1]c_b^2}{eq(R)Q} \quad (3a)$$

$$W(F_1=J+\tfrac{1}{2}\leftrightarrow F_1=J-\tfrac{1}{2})=-\frac{3}{4}\frac{eq(R)Q(2J+1)}{(2J+3)(2J-1)}+c_a(J+\tfrac{1}{2})+\frac{c_b}{J}[\pm1-\tfrac{3}{4}] \quad (3b)$$

$$W(F_1=J-\tfrac{1}{2}\leftrightarrow F_1=J-\tfrac{3}{2})=\frac{eq(R)Q}{4}+c_a(J-\tfrac{1}{2})+\frac{c_b}{J}[\mp1+\tfrac{3}{4}]+\frac{3[1\mp1]c_b^2}{eq(R)Q}, \quad (3c)$$

where $W(F_1+1\leftrightarrow F_1)=E(F_1+1)-E(F_1)$, $F=F_1+i_b$, and $(\pm)$ refer to $i_b=\pm\frac{1}{2}$.

Since $c_b\sim73$ kc,[12] $eqQ\sim15$ Mc, and the most probable $J=55$ (see Sec. II), the contribution of the second

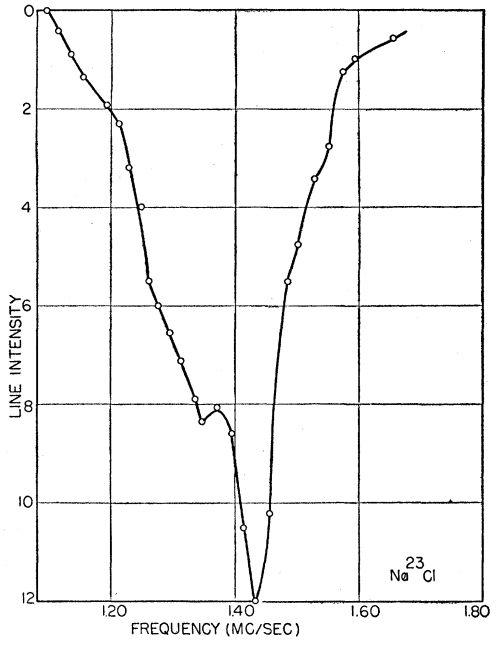

FIG. 4. Zero field spectrum of Na^{23} in $Na^{23}Cl$. Peak intensity corresponds to a 0.8-percent decrease in total beam. Radiofrequency current was 10 amperes.

[10] E. U. Condon and G. Shortley, *Theory of Atomic Spectra* (Cambridge University Press, London, 1935), Chapter III.

[11] See reference 10, Chapter II.

[12] Carlson, Lee, and Fabricand, Phys. Rev. **85**, 784 (1952).

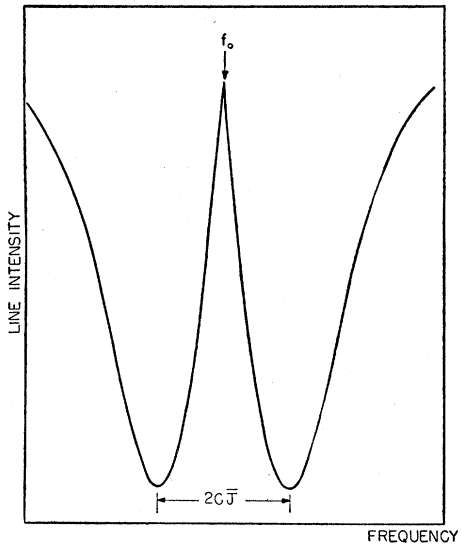

FIG. 5. The effect of the cJ term on a zero field line, assuming no other v or J dependence. f_0 marks the frequency at which the single resonance line would fall if there were no $\mathbf{I}\cdot\mathbf{J}$ interaction. The frequencies of the peaks of the wings are given by $f_1=f_0+c\bar{J}$, $f_2=f_0-c\bar{J}$, where $\bar{J}$ is the most probable J in the oven source. The splitting, neglecting all other effects, is then given by $2c\bar{J}$. This figure is a graphical representation of step 2 in the line shape analysis of Sec. C.

nucleus to the transition energies is negligibly small for most molecules in the beam. The effect of the second nucleus is considered in Appendix II.

For large J, the J dependence in (3b) gives a low frequency transition which is not observed in this experiment. The observed zero field spectra are due to the transitions (3a) and (3c).

B. Variation of eqQ with Vibration and Rotation

It has previously been observed[13] in molecular beam electric resonance experiments that eqQ varies approximately linearly with vibrational state, with about a 1 percent variation per state. For $TlCl^{35}$, Carlson, Lee, and Fabricand[12] find that this variation is (0.5 ± 1) percent.

Such a variation can be explained by assuming that q varies with R during the course of the molecular vibration, as assumed in Sec. A above, with

$$q(R)=q^{(0)}+q^{(1)}[(R-R_e)/R_e] +q^{(2)}[(R-R_e)/R_e]^2+\cdots. \quad (4)$$

R_e is the equilibrium internuclear distance in the state $v=0$, $J=0$. The coefficients $q^{(0)}$, $q^{(1)}$, $q^{(2)}$, $\cdots$ are assumed to be of the same order of magnitude to ensure the convergence of (4). It is interesting that the theoretical calculations of Nordsieck and Newell[14] for q in the deterium molecule give values of $q^{(0)}=1.15\times10^{15}$, $q^{(1)}=-5.50\times10^{15}$, and $q^{(2)}=13.0\times10^{15}$, in esu all the same order of magnitude. It is shown in Appendix III that the average value of expansion (4) over the molecular rotation and vibration is of the form:

$$q=q^{(0)}+q^{(J)}J(J+1)+q^{(v)}(v+\tfrac{1}{2}) \quad (5)$$

where

$$q^{(J)}=(2B_e/\omega_e)^2q^{(1)},$$

and

$$q^{(v)}=\left[3\left(\frac{B_e}{\omega_e}\right)\left(1+\frac{\alpha_e\omega_e}{6B_e^2}\right)q^{(1)}+2\left(\frac{B_e}{\omega_e}\right)q^{(2)}\right]$$

and B_e, ω_e, α_e, are the usual molecular constants[15] in units of cm^{-1}.

This average not only describes the linear variation of eqQ with vibrational quantum number, but also predicts a quadratic variation of eqQ with rotational quantum number. As will be seen in Sec. V, an analysis of the zero field line shape of $TlCl^{35}$ and $TlCl^{37}$, assuming a rotational and vibrational variation, can be made to explain the observed spectra rather well. The values of $eq^{(0)}Q$, $eq^{(1)}Q$, and $eq^{(2)}Q$ obtained will be consistent with the assumption that $q^{(0)}$, $q^{(1)}$, $q^{(2)}$ are all of the same order of magnitude. While $q^{(J)}$ and $q^{(v)}$ have a slight dependence on isotope through the rotational and vibrational constants, $q^{(0)}$, $q^{(1)}$, and $q^{(2)}$ are the same for different isotopes in the same molecule.

C. Line Shape

If we neglect the terms due to c_b, and replace $q(R)$ in (3a) and (3c) by q of (5), we obtain for the observed transition frequencies:

$$f_1=f_0+Pv+gJ^2-CJ, \quad f_2=f_0+Pv+gJ^2+CJ \quad (6)$$

where

$$f_0=(eq^{(0)}+\tfrac{1}{2}eq^{(v)})Q/4h\equiv e\bar{q}Q/4h, \quad P=eq^{(v)}Q/4h,$$
$$g=eq^{(J)}Q/4h, \quad c=c_a/h.$$

In (6) we have neglected small v and J independent terms of order $|c_a|/h$, since $|c_a|/h$ is only about 1 kilocycle; and we have neglected gJ compared to cJ, since $g\ll c$. Also, $e\bar{q}Q$ has been assumed positive for convenience. We cannot deduce the sign of $e\bar{q}Q$ from our observations, though Carlson, Lee, and Fabricand[12] are able to determine the sign. The v and J independent part of (6) is not $eq^{(0)}Q$, but $e\bar{q}Q$, which is only very slightly different.

For convenient analysis of the zero field line shape, we neglect rf line broadening and other small effects, and reconstruct the line by the following steps:

1. With no v or J dependence, we have two superposed resonance curves, whose half-widths are determined by the resolution properties of the apparatus.

[13] L. Grabner and V. Hughes, Phys. Rev. **79**, 819 (1950).

[14] A. Nordsieck, Phys. Rev. **58**, 310 (1940); G. F. Newell, Phys. Rev. **78**, 711 (1950).

[15] G. Herzberg, *Spectra of Diatomic Molecules* (D. Van Nostrand Company, Inc., New York, 1950), second edition.

2. The cJ terms cause a linear displacement of f_1 and f_2 with J. Because of the close spacing of the levels for successive values of J, the transitions for individual J values will not be separately resolved, and a pair of structures will result, one for f_1 and one for f_2. The distribution of J states in the beam is given approximately by:

$$N(J)dJ\sim(2J+1)\exp[-\tfrac{1}{2}\alpha^2J(J+1)]$$
$$\sim J\exp(-\tfrac{1}{2}\alpha^2J^2) \text{ for large } J, \quad (7)$$

where

$$\alpha^2=2B_ehc/kT=1/\bar{J}^2.$$

$\bar{J}$ is the most probable J of the beam, and B_e is the rotational constant of the molecule.[15] The wings corresponding to f_1 and f_2 are symmetric about f_0, with a shape function given by the rotational distribution $N(J)$ (Fig. 5). Since the rotational distribution has its maximum at $J=\bar{J}$, the splitting between the wings is $2c\bar{J}$. If the sign of c were reversed, the roles of f_1 and f_2 would be reversed, and there would be no change in the observed spectrum.

3. The effect of gJ^2 will be to spread the wing where c and g are of the same sign (the additive wing) still further, and to narrow the wing where they are of opposite sign (the subtractive wing). This will give an observable asymmetry in the two wings, even though $g\ll c$, because g appears as gJ^2 while c appears as cJ. For large enough J, for the subtractive wing, gJ^2 will overcome the effect of cJ, and the wing will fold back on itself (Fig. 6). If $q^{(0)}$ and $q^{(J)}$ are of opposite sign, the subtractive wing will fall at higher frequencies; if $q^{(0)}$ and $q^{(J)}$ are of the same sign, the subtractive wing will fall at lower frequencies.

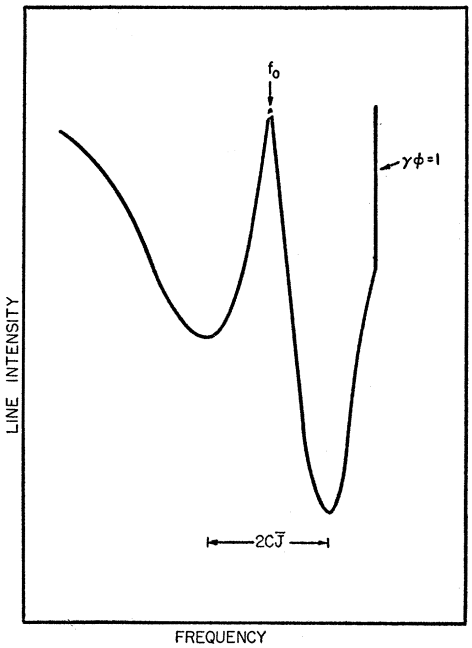

FIG. 6. The effect of the gJ^2 term on the curve of Fig. 5, as discussed in step 3 of Sec. C. The additive wing in this instance is the low frequency wing. For large J, the subtractive wing will fold back on itself, as is indicated here by the high frequency cutoff, at $\gamma\phi=1$.

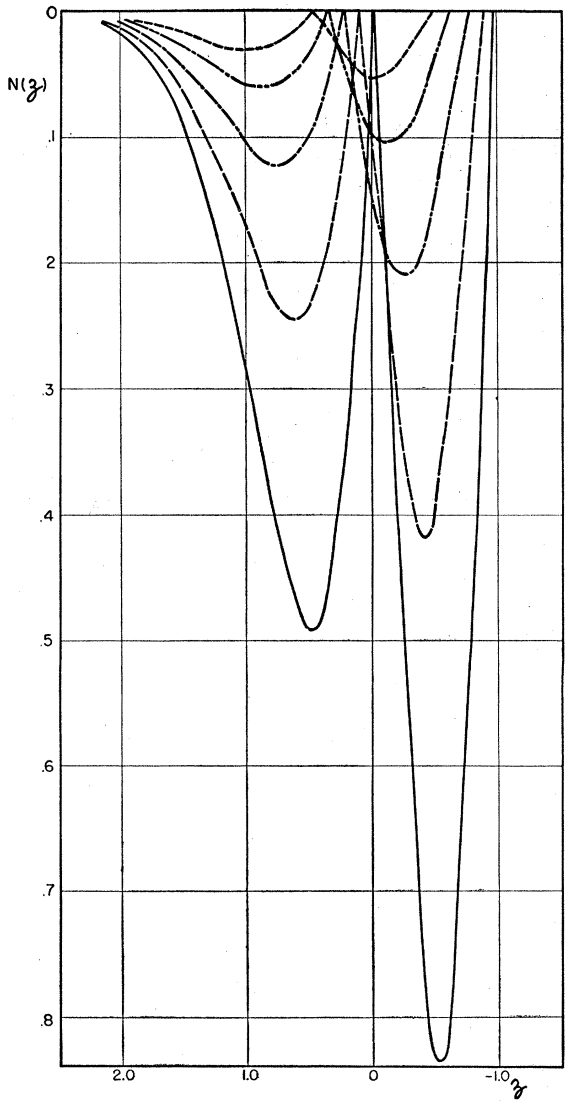

FIG. 7. The effect of the term Pv in Eq. (6), corresponding to step 4 in the line shape analysis. A series of curves of the form of Fig. 6 is found, each shifted in frequency by an amount Pv. The curves shown here are for $\gamma=0.30$. Their envelope, given in Fig. 9, gives best agreement with the experimentally observed resonance curves of TlCl^{35} and TlCl^{37}, shown in Figs. 1 and 2. $N(z)=\phi\exp(-\frac{1}{2}\phi^2)/|1\mp\gamma\phi|$, where $z=\pm\phi+\frac{1}{2}\gamma\phi^2=h(f-f_0)/c_a\bar{J}$.

4. The ratio of populations of successive vibrational states for a diatomic molecule is $\exp(-hc\omega_e/kT)$, where ω_e is the vibrational constant of the molecule.[15] The term Pv in (6) thus gives a series of pairs of wings, as in (3), of relative intensity $\exp(-hc\omega_e/kT)$, each shifted in frequency by an amount Pv (Fig. 7). If $q^{(0)}$ and $q^{(v)}$ are of opposite sign, the vibrational shift is down in

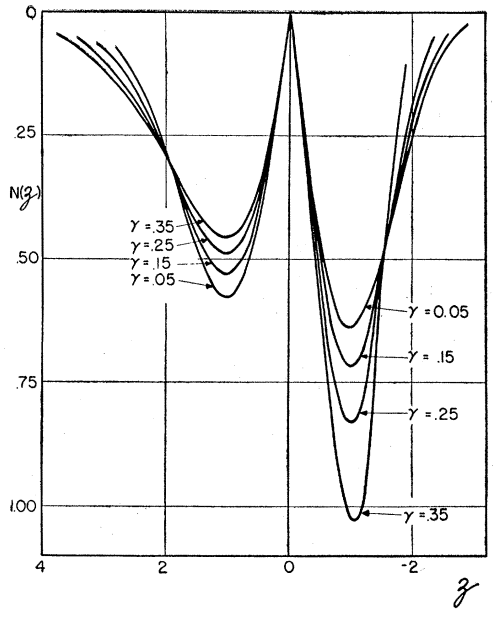

FIG. 8. $N(z)$ *vs* z for various values of the parameter γ, where $\gamma=(\bar{J}/2c_a)eq^{(J)}Q$, $z=h(f-f_0)/c_a\bar{J}$. (See definitions (9).)

frequency; if $q^{(0)}$ and $q^{(v)}$ are of the same sign, the vibrational shift is up in frequency. If $|P|$ is appreciably less than $|c|J$, and the decrease in population per vibrational state is large, then the vibrational structure will not be resolved. This turns out to be the case for $TlCl^{35}$ and $TlCl^{37}$. We obtain a shape function for the frequencies of (6), neglecting the vibrational superposition due to the term Pv. The latter effect has to be considered separately for each case. The distribution function (7) is transformed from J variables to f variables:

$$N(f)df=N(J)|dJ/df|df$$
$$=J\exp(-\tfrac{1}{2}\alpha^2J^2)df/|\pm c+2gJ|, \quad (8)$$

where the (+) and (−) refer to f_1 and f_2, respectively. We introduce the parameters:

$$\phi=\alpha J=J/\bar{J} \quad (9)$$
$$z=\alpha(f-f_0)/c=(f-f_0)/c\bar{J}=\pm\phi+(g/c\alpha)\phi^2,$$
from (6)
$$g/c\alpha=\gamma/2$$

(8) then gives

$$N(z)\sim\phi\exp(-\tfrac{1}{2}\phi^2)/|1\mp\gamma\phi| \quad (10)$$

where $z=\pm\phi+\frac{1}{2}\gamma\phi^2$.

$N(z)$ *versus* z is plotted in Fig. 8 for several values of the parameter γ. A small value of g is enough to produce a considerable asymmetry. For example, when $\gamma=0.25$, the ratio of the peak intensities of the wings is 1.7:1. If $\bar{J}$ is about 40, this corresponds to g/c of 6×10^{-3}. Because of the large value of $\bar{J}$, c and g can be determined fairly accurately, since the line splitting is about $2c\bar{J}$, and γ is proportional to $\bar{J}$.

The subtractive wing shows a discontinuity at $\gamma\phi=1$. The density function goes to infinity at this point, but for $\gamma\lesssim0.4$, the integrated area at the discontinuity is so small that the line is not affected appreciably.

V. ANALYSIS OF $TlCl^{35}$ AND $TlCl^{37}$ CURVES

The spectra of $TlCl^{35}$ and $TlCl^{37}$ are analyzed, using the theory of the previous section. The value of $\gamma=2g/c\alpha$, in the notation of the previous section, is selected so that, when used in conjunction with a known value of $eq^{(v)}Q$,[12] the composite curve resulting from a graph of $N(z)$ *versus* z for several vibrational states will agree as closely as possible with the experimental curve. In the case of $TlCl^{35}$ and $TlCl^{37}$, a value of $\gamma=0.25$ was found to give the best fit. The reason the same value of γ serves for both isotopes is that

$$\frac{\gamma^{35}}{\gamma^{37}}\sim\left(\frac{g}{c}\right)^{35}\Big/\left(\frac{g}{c}\right)^{37}\sim\left(\frac{Q}{\mu}\right)^{35}\Big/\left(\frac{Q}{\mu}\right)^{37}$$

(μ is the nuclear magnetic dipole moment), and this ratio is very close to one. There are two isotopes of Tl, Tl^{203}, and Tl^{205}, but both have spin $\frac{1}{2}$ and almost identical masses, so that the spectra of Cl for these two isotopes of Tl are the same.

The factor for the decrease in line intensity for successive vibrational states is 0.50. With a value of $eq^{(v)}Q$ equal to $0.006e\bar{q}Q$, which is close to the value of $(0.005\pm0.001)e\bar{q}Q$ given by the results of the electric resonance method,[12] the curves corresponding to the states $v=0$, 1, 2, 3, and 4 are plotted in Fig. 7. The envelope of these curves is shown in Fig. 9, together with a set of experimental points for $TlCl^{37}$. The ratio of the half-widths of the wings is 1.75, as compared with an average of 1.8 for the experimentally observed minima; the ratio of the intensities is 0.62 as compared with an average of 0.7 for the observed minima. The difference between the calculated and experimental ratio of intensities may be explained by rf broadening effects, and by the difficulty inherent in observing the peak intensity for a narrow resonance line.

The value of $|c_a|/h$ is obtained by noting the separation between the split peaks of the zeroth vibrational line. $|e\bar{q}Q|/h$ is then determined as the mean between these two peaks. The value of $eq^{(J)}Q/h$ is obtained by solving for g in the equation $g=c\alpha\gamma/h$. The results obtained from this analysis of $TlCl^{35}$ and $TlCl^{37}$ are given in Table I.

The splitting due to the $\mathbf{I}_a\cdot\mathbf{J}$ interaction can be expressed as that due to an equivalent magnetic field at the chlorine nucleus due to the rotation of the molecule as a whole. The magnitude of the magnetic field per rotational quantum number H_a is given by $H_a=|c_a/g_I\mu_N|$. The value of c_a for $Cl^{35}=1.4$ kc,

equivalent to $H_a=3.4$ gauss; the value of c_a for Cl^{37} is 1.1 kc, equivalent to $H_a=3.2$ gauss.

The sign of $eq\bar{q}Q$ has been found to be negative, the sign of c_a to be positive.[12] Since the resonance curve tapers off gradually at high frequencies, $eq^{(v)}Q$ has the same sign as $eq\bar{q}Q$. Since the high frequency wing is broadened by the effect of the rotational variation, as discussed in Sec. IV C, $eq^{(J)}Q$ has the same sign as $eq\bar{q}Q$. In other molecules in which results are available (CsF,[16] RbF,[17] KF[13]), $eq^{(v)}Q$ and $eq\bar{q}Q$ have opposite signs.

The criteria for the validity of the expansion of $q(R)$ given in Eq. (4) are given in Eq. (20) of Appendix III as:

$$\begin{aligned}&(\Delta R/R_e)_{\text{rot}}=(2B_e/\omega_e)^2\bar{J}(\bar{J}+1)\ll 1\\&(\Delta R/R_e)_{\text{vib}}=(B_e/\omega_e)^{\frac{1}{2}}\ll 1 \quad \text{for } J=\bar{J}, \text{ and } v=0.\end{aligned} \tag{11}$$

For TlCl^{35}, $B_e\sim 0.0873$ cm^{-1}, $\omega_e=287.47$ cm^{-1}, $\alpha_e=4.3\times 10^{-4}$ cm^{-1},[18] $\bar{J}=55$. Substituting in Eqs. (11), we obtain:

$$\begin{aligned}(\Delta R/R_e)_{\text{rot}}&=11.4\times 10^{-4},\\(\Delta R/R_e)_{\text{vib}}&=1.74\times 10^{-2},\end{aligned} \tag{12}$$

TABLE I. Experimental values for molecular constants in the molecules TlCl^{35}, TlCl^{37}, Na^{23}F, and Na^{23}Cl.[a]

Molecule	eqQ/h Mc	c_a/h kc	H_a gauss	$eq^{(v)}Q/h$ kc	$eq^{(J)}Q/h$ cycles/sec
TlCl^{35}	(−)15.788±0.02	(+)1.4±0.1	3.4±0.3	−96	−18.4
TlCl^{37}	(−)12.425±0.02	(+)1.1±0.1	3.2±0.3	−76	−16.4
Na^{23}F	8.40 ±0.02	~1	~1	+80	+32
Na^{23}Cl	5.61 ±0.02	~1	~1	+88	+24

[a] Signs for eqQ/h for TlCl^{35} and TlCl^{37} are from reference 12. Signs for c_a/h for TlCl^{37} and TlCl^{35} are from reference 18.

from which we infer that for TlCl^{35} the expansion of $q(R)$ given in Eq. (4) is valid. For TlCl^{35} the experimental values which are used to obtain $eq^{(0)}Q$, $eq^{(1)}Q$, and $eq^{(2)}Q$ are:

$$\begin{aligned}e\bar{q}Q/h&=-15.788\times 10^6 \text{ cycles/sec},\\eq^{(v)}Q/h&=-96\times 10^3 \text{ cycles/sec},\\eq^{(J)}Q/h&=-18.4 \text{ cycles/sec}.\end{aligned}$$

From the relationships of (5) and the definition of $\bar{q}$ in (6), we obtain:

$$\begin{aligned}eq^{(0)}Q/h&=-15.740\times 10^6 \text{ cycles/sec},\\eq^{(1)}Q/h&=-49.6\times 10^6 \text{ cycles/sec},\\eq^{(2)}Q/h&=+100\times 10^6 \text{ cycles/sec}.\end{aligned}$$

In the case of TlCl^{35}, then, the assumption that $|q^{(0)}|\sim|q^{(1)}|\sim q^{(2)}|$ is justified.

[16] J. W. Trischka, Phys. Rev. **74**, 718 (1948).
[17] V. Hughes and L. Grabner, Phys. Rev. **79**, 314 (1950).
[18] Carlson, Lee, and Fabricand, private communication.

The results for TlCl^{37} are obtained in a similar manner, and the constants for both TlCl^{35} and TlCl^{37} are given in Table I.

VI. ANALYSIS OF Na^{23}Cl AND Na^{23}F CURVES

An analysis similar to that of the spectrum of TlCl is performed for the observed zero field lines of Na^{23}Cl and Na^{23}F. Since the splitting in the latter cases is not as prominent, less sensitive criteria are used to guide the choice of constants in constructing the line shapes. Thus the ratio of intensities of the two wings, and the ratio of the half-width of the composite line to the splitting are used in the selection of values of γ and of $eq^{(v)}Q$ which lead to a line shape similar to that experimentally observed. The value of ω_e is not known for Na^{23}F, but an empirical estimate gives $\omega_e=530$, so that the decrease in line intensity with vibrational state is 0.53. Values of $\gamma=0.25$ and $eq^{(v)}Q=0.01e\bar{q}Q$ are found to give the best fit. The line, constructed as described in Sec. IV C, then has for the ratio of intensities 1.22, as compared with 1.25 actually observed for Na^{23}F; and for the ratio of half-width of composite line to splitting 2.1, compared with 2.4 actually observed.

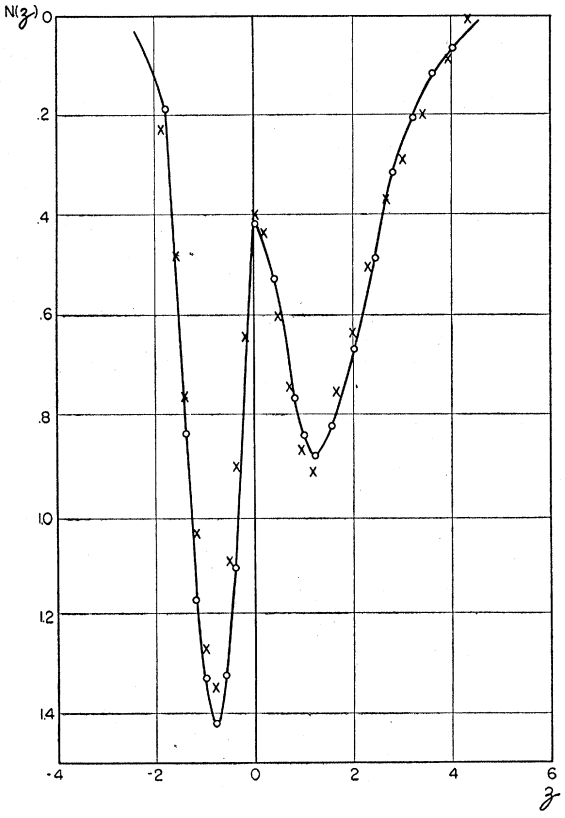

FIG. 9. Envelope of the curves of the first five vibrational states for TlCl given in Fig. 7. γ was taken to be 0.30 for best agreement with the experimental resonance curves for TlCl^{35} and TlCl^{37}. For purposes of comparison, the experimental points of the TlCl^{37} resonance in Fig. 2 are indicated here by crosses.

The values of the constants obtained are listed in Table I. The zero field value of $e\bar{q}Q$ for Na in $Na^{23}F$, 8.40 Mc, is to be compared with the high field value of 8.12 Mc, obtained by Logan and Coté.[19] The 3 1/2 percentage discrepancy between these results is consistent with similar discrepancies found in the other sodium halides.[4] This effect in the sodium halides will be discussed more fully in the following section.

In the case of Na^{23} in $Na^{23}Cl$, the decrease of line intensity with vibrational state is 0.58, and the values of γ and $eq^{(v)}Q$ which give the best fit are again $\gamma=0.25$ and $eq^{(v)}Q=0.01e\bar{q}Q$. The ratio of intensities of the wings is 1.36, as compared with the experimentally observed ratio of 1.43; while the ratio of the half-width of the composite line to the splitting, 1.9, is to be compared with the experimentally observed ratio of 2.0. The constants obtained from an analysis of the $Na^{23}Cl$ line are listed in Table I. The signs of $eq^{(v)}Q$ and $eq^{(J)}Q$ are found to be opposite to the sign of $e\bar{q}Q$ for both $Na^{23}F$ and $Na^{23}Cl$.

In the analysis of the line shape of $Na^{23}F$ we have neglected the effect of an $\mathbf{I}_b\cdot\mathbf{J}$ interaction for fluorine; and in the case of $Na^{23}Cl$, we have neglected both the quadrupole interaction and $\mathbf{I}_b\cdot\mathbf{J}$ interaction of chlorine. As indicated in Appendix II, $e\bar{q}Q$ for Cl in $Na^{23}Cl$ would have to be greater than 3.2 Mc to affect the line shape. The values of c_b for F in $Na^{23}F$ and Cl in $Na^{23}Cl$ would have to be about 100 kc or more to affect the line shapes. However, $e\bar{q}Q$ for Cl in KCl is 420 kc,[19] which should not be much different from $e\bar{q}Q$ for NaCl; while the known values of $\mathbf{I}_b\cdot\mathbf{J}$ for the alkali halides observed experimentally[17] are of the order of 10 kc. It is highly probable, therefore, that these constants are not large enough to affect the sodium spectra in NaF and NaCl. Furthermore, the line shapes can be reasonably well explained without assuming their presence.

Because the molecular constants of NaCl and NaF are not well known, and because of the large possible error in determining $eq^{(v)}Q$ and $eq^{(J)}Q$ for these molecules, we cannot determine the constants $eq^{(1)}Q$ and $eq^{(2)}Q$ with any degree of precision. However, an estimate indicates that they are of the same order of magnitude as $eq^{(0)}Q$.

VII. DISCUSSION

From the zero field magnetic resonance spectra of $TlCl^{35}$ and $TlCl^{37}$, the ratio of the quadrupole interactions is found to be:

$$|e\bar{q}Q(Cl^{35})|/|e\bar{q}Q(Cl^{37})| = 15.788/12.425 = 1.270\pm0.005.$$

The electric resonance method gives the result:

$$|e\bar{q}Q(Cl^{35})|/|e\bar{q}Q(Cl^{37})| = 1.2691\pm0.0005.$$

These results and the results of recent atomic beam[20] and microwave[21] measurements of the chlorine-quadrupole-moment-ratios all agree within limits of experimental error.

It is interesting to note that the quantity $e\bar{q}$, which normally enters into the experimentally measured quadrupole coupling, is not the same for two isotopes in the same molecule because of different zero point vibration for the two isotopes. A simple calculation shows that the error introduced by this effect into the quadrupole moment ratio is about 1 in 14,000 for TlCl, negligible for these experiments. The ratio of the magnitude of c_a for $TlCl^{35}$ to c_a for $TlCl^{37}$ is:

$$|c_a(Cl^{35})|/|c_a(Cl^{37})| = 1.4/1.1 = 1.25\pm0.10.$$

The Foley and Wick[9] theories of the $\mathbf{I}\cdot\mathbf{J}$ interaction explain the effect as due to the coupling of the nuclear magnetic moment with the internal magnetic fields of the molecule. On this model, or, in fact, on any reasonable model, the constant c_a would be expected to be proportional to the nuclear magnetic moment for isotopes in the same molecule. The ratio of the magnetic moments of Cl^{35} and Cl^{37} is $\mu(Cl^{35})/\mu(Cl^{37})=1.21$,[22] in good agreement with the ratio of $|c_a(Cl^{35})|/|c_a(Cl^{37})|$. This gives further support for assuming that the split line in TlCl is actually due to an $\mathbf{I}\cdot\mathbf{J}$ interaction.

Nierenberg and Ramsey[4] point out that there exists a 5-percent discrepancy between the values of the quadrupole coupling obtained at zero field and at high field. They are able to explain about $\frac{1}{3}$ of this discrepancy by a refinement of the analysis of the high field line, taking into account resolution and the distribution of J states in the beam. Another small fraction of the discrepancy may be explained by the fact that they took the position of the zero field quadrupole resonance to be at the position of the highest peak. The actual zero field quadrupole resonance corresponds more nearly to the midpoint between the highest peak, for the subtractive wing, and the lower secondary peak for the additive wing (which, in the case of the sodium halides is barely resolved). After these effects have been considered, there still remains a small discrepancy between the zero and high field values, which can perhaps be explained by considering the effect of the rotational and vibrational variations of eqQ on the high field spectrum.

We are grateful to Professor I. I. Rabi for suggesting this problem, and for his guidance throughout the course of the experiment. We are greatly indebted to Professor T. Y. Wu for his help and encouragement during the early stages of the experiment. We also wish to thank the members of the molecular beams laboratories, and Professors C. H. Townes and H. M. Foley for several helpful suggestions.

[19] Logan, Coté, and Kusch, private communication.
[20] V. Jaccarino and J. G. King, Phys. Rev. **83**, 471 (1951).
[21] R. Livingston, Phys. Rev. **82**, 289 (1951).
[22] F. Bitter, Phys. Rev. **75**, 1326 (1949); H. Taub and P. Kusch, Phys. Rev. **75**, 1481 (1949).

APPENDIX I. ZERO FIELD ENERGY LEVELS FOR $I_a=\frac{3}{2}$, $I_b=\frac{1}{2}$

The matrix elements of $(\mathbf{I}_a\cdot\mathbf{I}_b)$ are calculated in the $(F, F_1, J, I_a, I_b, M_F)$ representation as:

$$\langle I_AJF_1I_bFM_F|\,\mathbf{I}_a\cdot\mathbf{I}_b\,|I_AJF_1I_bFM_F\rangle=\frac{1}{2}\left\{\frac{I_a(I_a+1)-J(J+1)+F_1(F_1+1)}{2F_1(F_1+1)}\right\}\{F(F+1)-F_1(F_1+1)-I_b(I_b+1)\}$$

$$\langle I_aJF_1-1I_bFM_F|\,\mathbf{I}_a\cdot\mathbf{I}_b\,|I_aJF_1I_bFM_F\rangle=\frac{[(F_1-I_a+J)(F_1+I_a-J+1)(F_1+I_a+J+1)(I_a+J+1-F_1)]^{\frac{1}{2}}\cdot[(F+F_1-I_b)(F+I_b-F_1+1)(F+I_b+F_1+1)(F_1+I_b-F)]^{\frac{1}{2}}}{4F_1[4F_1^2-1]^{\frac{1}{2}}} \tag{13}$$

$$\langle I_aJF_1+1I_bFM_F|\,\mathbf{I}_a\cdot\mathbf{I}_b\,|I_aJF_1I_bFM_F\rangle=\frac{[(F_1-I_a+J+1)(F_1+I_a-J+1)(F_1+I_a+J+2)(I_a+J-F_1)]^{\frac{1}{2}}\cdot[(F+F_1-I_b+1)(F+I_b-F_1)(F+I_b+F_1+2)(F_1+I_b-F+1)]^{\frac{1}{2}}}{4(F_1+1)[4(F_1+1)^2-1]^{\frac{1}{2}}}.$$

The perturbation H_1 is $[-c_b(\mathbf{I}_a\cdot\mathbf{I}_b)]$. From (13), the first-order perturbation $E^{(1)}$ is of order $|c_b|$. The energy denominator appearing in the second-order perturbation energy $E^{(2)}$ is

$$E(F_1, F)-E(F_1+1, F)\sim-\frac{3}{8}\frac{eqQ(2J+2i_a+2)}{I_a(2I_a-1)(2J+3)(2J-1)}[(4i_a+2)J+2i_a(i_a+2)-2I_a(I_a+1)+3]-c_aJ+c_bJ, \tag{14}$$

for large J.

From (14), we see that, for large J, the second-order perturbation energy $E^{(2)}$ is of order $|c_b|^2/|eqQ|$ for $i_a\neq-\frac{1}{2}$; in the case when $i_a=-\frac{1}{2}$, $E^{(2)}\sim|c_b|^2/|c_b|J$.

Note, the perturbation calculation may diverge for $i_a=-\frac{1}{2}$ when (14) is zero. However, if this does occur at all, it occurs for fairly low J, and (14) remains small only for a few J states, so that the effect on the line shape should be small.

The energy levels for large J, up to order $E^{(2)}$, are:

$$E(F_1=J+\tfrac{3}{2})=\frac{-eqQ}{8(2J+3)(2J-1)}\{9J^2+3J-5J(J+1)\}+\frac{3c_aJ}{2}+\frac{c_b}{2}\left\{\pm J\pm\frac{1}{2}-\frac{1}{2}\mp\frac{3}{4J}+\frac{3}{4J}\right\}-\frac{3[\frac{1}{2}\mp\frac{1}{2}]c_b^2}{eqQ}$$

$$E(F_1=J+\tfrac{1}{2})=\frac{-eqQ}{8(2J+3)(2J-1)}\{J^2-5J+6-5J(J+1)\}+\frac{c_a}{2}(J-3)+\frac{c_b}{2}\left\{\pm J\pm\frac{1}{2}-\frac{1}{2}\mp\frac{3}{4J}-\frac{3}{4J}\right\}+\frac{3[\frac{1}{2}\mp\frac{1}{2}]c_b^2}{eqQ}$$

$$E(F_1=J-\tfrac{1}{2})=\frac{-eqQ}{8(2J+3)(2J-1)}\{J^2+7J+12-5J(J+1)\}$$
$$+c_a(-J-4)+\frac{c_b}{2}\left\{\pm J\pm\frac{1}{2}-\frac{1}{2}\mp\frac{11}{4J}+\frac{3}{4J}\right\}+\frac{3[\frac{1}{2}\mp\frac{1}{2}]c_b^2}{eqQ} \tag{15}$$

$$E(F_1=J-\tfrac{3}{2})=\frac{-eqQ}{8(2J+3)(2J-1)}\{9J^2+15J+6-5J(J+1)\}$$
$$+\frac{c_a}{2}(-3J-3)+\frac{c_b}{2}\left\{\pm J\pm\frac{1}{2}-\frac{1}{2}\mp\frac{3}{4J}-\frac{3}{4J}\right\}-\frac{3[\frac{1}{2}\mp\frac{1}{2}]c_b^2}{eqQ}$$

where the $(\pm)$ refer to $i_b=\pm\frac{1}{2}$.

These energy levels give the transition energies of (3).

APPENDIX II. EFFECT OF SMALL PERTURBATIONS ON THE LINE SHAPE

To test whether a perturbation term of the form K_nJ^n affects the line shape, we will calculate the shape function neglecting the terms gJ^2 and Pv. The frequencies f_1 and f_2 of (6) then become:

$$f_1=f_0-cJ+K_nJ^n,\quad f_2=f_0+cJ+K_nJ^n \tag{16}$$

where K_n is assumed to have the same sign in f_1 and f_2 to produce the maximum possible line asymmetry. By a series of steps analogous to those of Eqs. (8)–(10), we obtain:

$$N(z)\sim\phi\exp(-\tfrac{1}{2}\phi^2)/|1\mp\gamma^n\phi^{n-1}|, \tag{17}$$

where

$$z=\pm\phi+(\gamma/n)\phi^n=(f-f_0)/c\tilde{J},\text{ and }\gamma_n=|nK_n/c\alpha^{n-1}|.$$

This reduces to Eq. (10) for $n=2$.

For a small value of K_n, the position and magnitude of the two peaks will not be much different from those

produced by cJ alone. Then, the peaks will occur when $\phi=1$, and the ratio of the two peaks will be:

$$R=(1-\gamma_n)/(1+\gamma_n). \tag{18}$$

We take as the condition for the neglect of a perturbation, that $(1-R)$ be less than 0.1. This gives as the condition for neglect,

$$|nK_n/c\alpha^{n-1}|<0.05. \tag{19}$$

The perturbations of interest will be of the form $K_{-1}J^{-1}$ and $K_{-2}J^{-2}$. These diverge for small values of J, giving rise to apparent discontinuities in the shape function. However, the perturbations are obtained in these cases, assuming J fairly large, while the discontinuities occur for low J. In addition, the density of states is low for small values of J. We will then take (19) as the criterion for neglect of a term, even for $n=-1$ and -2.

The perturbations we consider are:

(1) The perturbations of order $\sim c_b/J$ in Eq. (3). The largest term of this form is $7c_b/4J$.

(2) The perturbation terms due to the off-diagonal matrix elements of the quadrupole operator. These are of order $|eqQ|^2/hcB_eJ$.

(3) Perturbations (in the case of NaCl) due to a quadrupole coupling eq_bQ_b of the second nucleus. These terms can be shown to contribute to the transition energies in order $\sim|eq_bQ_b|/J^2$.

For TlCl, $c_b\sim 75$ kc,[12] $eqQ\sim 15$ Mc, $B_e\sim 0.087$ cm^{-1}, $c_a\sim 1$ kc, $\bar{J}=55$. For perturbation (1), TlCl gives $\gamma_{(1)}=|7c_b/c_a4\bar{J}^2|\sim 0.043$. The exact evaluation of perturbation (2) requires a rather lengthy calculation. However, the fact that the zero field electric resonance spectrum of TlCl can be well explained without considering these terms indicates that the terms are at most a few kc. Assuming perturbation (2) to be about 10 kc/sec/J, $\gamma_{(2)}=|10\text{ kc/sec}/c_aJ^2|\sim 0.003$. For NaCl, $c_a\sim 1$ kc, $\bar{J}\sim 40$. There are no data available on the quadrupole coupling of chlorine, eq_bQ_b, in NaCl. However, from (19), the effect of the chlorine on the spectrum of sodium in NaCl is negligible if $|eqQ|<3.2$ Mc.

APPENDIX III. ROTATIONAL AND VIBRATIONAL VARIATION OF q

As in Eq. (4), we take $q(R)$ to be a function of the form:

$$q(R)=q^{(0)}+q^{(1)}[(R-R_e)/R_e]+q^{(2)}[(R-R_e)/R_e]^2+\cdots.$$

For this expansion to converge rapidly, the coefficients $q^{(0)}$, $q^{(1)}$, $q^{(2)}$, $\cdots$ must be of the same order of magnitude, and the change in R during the course of the molecular vibration and rotation must be much less than R_e. A semiclassical argument gives

$$(\Delta R/R_e)_{\text{rot}}=(2B_e/\omega_e)^2J(J+1),$$
$$(\Delta R/R_e)_{\text{vib}}=(2B_e/\omega_e)^{\frac{1}{2}}(v+\tfrac{1}{2})^{\frac{1}{2}},$$

so that the criteria for the validity of the expansion are:

$$(2B_e/\omega_e)^2J(J+1)\ll 1,\quad (2B_e/\omega_e)^{\frac{1}{2}}(v+\tfrac{1}{2})^{\frac{1}{2}}\ll 1. \tag{20}$$

To average $q(R)$ over vibration and rotation, we must use appropriate vibrator-rotator wave functions. A general molecular vibrator potential is assumed of the form,

$$V(R)=K_2[(R-R_e)/R_e]^2+K_3[(R-R_e)/R_e]^3+K_4[(R-R_e)/R_e]^4+\cdots. \tag{21}$$

The wave functions for this potential are obtained, solving a harmonic oscillator problem, with $K_3[(R-R_e)/R_e]^3+K_4[(R-R_e)/R_e]^4+\cdots$ as perturbations. The average of $q(R)$ then becomes,

$$q=q^{(0)}+(2B_e/\omega_e)^2q^{(1)}J(J+1)+[-3q^{(1)}(B_e/\omega_e)(K_3/K_2)+2q^{(2)}(B_e/\omega_e)](v+\tfrac{1}{2}). \tag{22}$$

To evaluate (K_3/K_2), a perturbation calculation of the energy for the potential of (21) is performed. Identifying the coefficient of the $(v+\frac{1}{2})J(J+1)$ term in the energy, as $(-\alpha_ehc)$,

$$\alpha_e=-\tfrac{3}{2}\omega_e(2B_e/\omega_e)^2[1+(K_3/K_2)]. \tag{23}$$

Substituting for (K_3/K_2) into (22),

$$q=q^{(0)}+(2B_e/\omega_e)^2q^{(1)}J(J+1)+[3q^{(1)}(B_e/\omega_e)\times(1+\alpha_e\omega_e/6B_e^2)+2q^{(2)}(B_e/\omega_e)]. \tag{24}$$

The relations (5) then follow from this.